



Tuning the structural stability and electronic properties of BiTe nanostructures-a density functional theory study

V. Nagarajan and R. Chandiramouli*

School of Electrical & Electronics Engineering, SASTRA University,
Tirumalaisamudram, Thanjavur -613 401, India

Abstract: The realistic nanostructures of pristine, Se and S incorporated BiTe nanostructures in the form of nanocone, nanosheet and nanotube are optimized and simulated successfully using density functional theory along with B3LYP/ LanL2DZ basis set. The formation energy, chemical potential and chemical hardness are used to study the structural stability of BiTe nanostructures. Point symmetry and dipole moment of pristine, Se and S incorporated BiTe nanostructures are also reported. The electronic properties of BiTe nanostructures are discussed in terms of ionization potential, electron affinity and HOMO-LUMO gap. The present work reveals that the incorporation of impurities leads in enhancing the structural stability and electronic properties of BiTe nanostructures, which find its application in power generator and gas sensors.

Keywords: bismuth telluride, nanostructure, formation energy, dipole moment, HOMO-LUMO.

Introduction

In recent days, converting heat energy into electricity has become a significant topic of research among the scientific community [1, 2]. Thus, the thermoelectric materials have attracted much interest among scientific community due to generating electricity under a temperature gradient. Especially, nanomaterials are considerable to improve the thermoelectric figure-of-merit owing to quantum confinement effects and enhancing surface phonon scattering [3]. Bismuth telluride (BiTe) compounds, including Bi_2Te_3 are the best thermoelectric materials among others [4]. Moreover, BiTe is frequently used in low temperature thermocouples, commercial solid state peltier coolers and in thermal energy scavenging [5]. Besides, BiTe is also one of the best thermoelectric materials with wide range of applications, such as in refrigerator [6], power generator [7] and as gas sensors [8]. It is a semiconductor with narrow band gap of 0.15 eV [9] which exhibits a rhombohedral crystal structure. Due to its predominant performance, BiTe is most often used for low-temperature thermoelectric devices. Different methods, including sputtering [10], flash evaporation [11], metal-organic chemical vapor deposition [12] and electrochemical deposition [13] have been extensively used to synthesis bismuth telluride thin films for the micro thermoelectric devices. Srinivasan et al., [14] proposed the texture development during deformation processing of the n-type bismuth telluride alloy $\text{Bi}_2\text{Se}_{0.3}\text{Te}_{2.7}$. Zeng et al., [15] reported the temperature and size effects on electrical properties and thermoelectric power of bismuth telluride thin films deposited by co-sputtering. Molli et al., [16] proposed the solvothermal synthesis and study of nonlinear optical properties of nanocrystalline thallium doped bismuth telluride. Density functional theory (DFT) is an efficient method to study the structural and electronic properties [17-19] of BiTe. The motivation behind the work is to fine-tune the structural stability and electronic properties of BiTe nanostructures with

substitution impurities. In the present work, structural stability of different BiTe nanostructures are studied and reported.

Computational methods

The pristine, S and Se substituted BiTe nanostructures in the form of nanosheet, nanotube and nanocone are optimized and simulated successfully with the help of Gaussian 09 package [20]. The atomic number of bismuth and tellurium is eighty three and fifty two respectively. In this work, different impurities are incorporated in pristine BiTe nanostructure and optimized. BiTe nanostructures are optimized with Becke's three-parameter hybrid functional (B3LYP) along with suitable LanL2DZ basis set [21-23]. While optimizing BiTe nanostructures, selection of the basis set is an important criterion. LanL2DZ basis set is a suitable choice for optimizing BiTe nanostructures along with pseudo potential approximation [24]. Moreover, LanL2DZ basis set is most suitable to Li-La, H and Hf-Bi elements. The density of states spectrum (DOS) of BiTe nanostructures are drawn using Gauss Sum 3.0 package [25].

Results and Discussion

The present work, mainly focus on dipole moment (DM), ionization potential (IP), chemical potential (CP), chemical hardness (CH), formation energy, HOMO-LUMO gap and electron affinity of BiTe nanostructures and the electronic properties of BiTe are fine-tuned with the incorporation of proper impurities such as selenium and sulfur. Figure 1 (a) – 1 (c) refers pristine, Se and S substituted BiTe nanocone respectively. The reason behind the selection of S and Se as impurity in the BiTe nanostructures are both S and Se are chalcogens like Te. Moreover, the substitution of S and Se modifies the electronic properties of BiTe nanostructures.

The different nanostructures of BiTe such as nanocone, nanosheet and nanotube are designed. The pristine structures of BiTe have nine Bi atoms and nine Te atoms. In the case of Se substituted BiTe nanostructures, there are nine Bi atoms, eight Te atoms and one Te atom is replaced with one Se atom. For S substituted BiTe nanostructures, nine Bi atoms, eight Te atoms are present and one Te atom is replaced with one S atom. The nanostructures of BiTe are shown in Figure 1 (a) – Figure 1 (i).

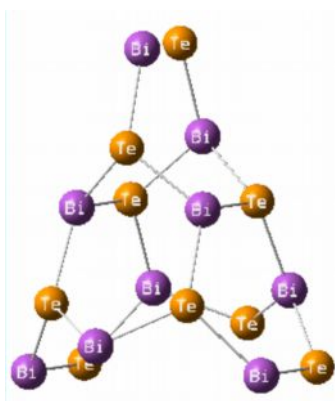


Figure. 1(a) pristine BiTe nanocone

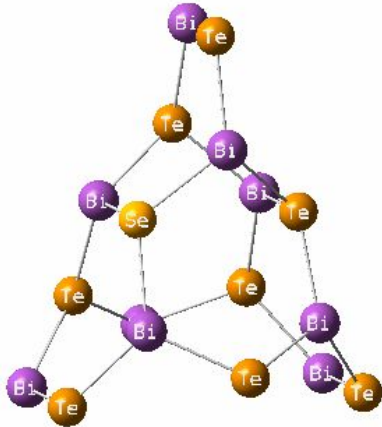


Figure. 1(b) Se substituted BiTenacone

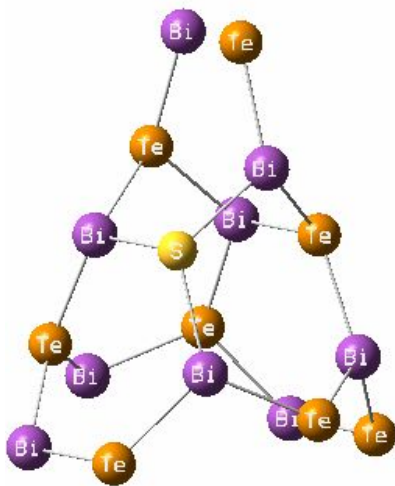


Figure. 1(c) S substituted BiTenacone

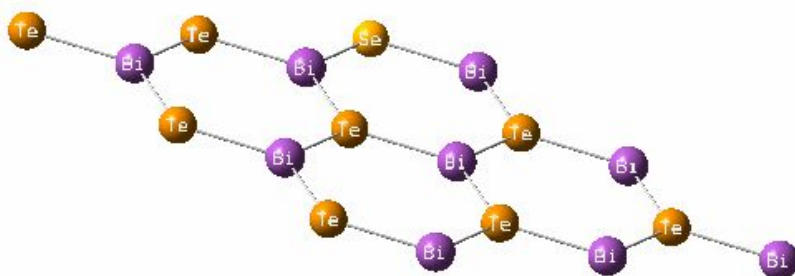


Figure. 1(d) pristine BiTenaosheet

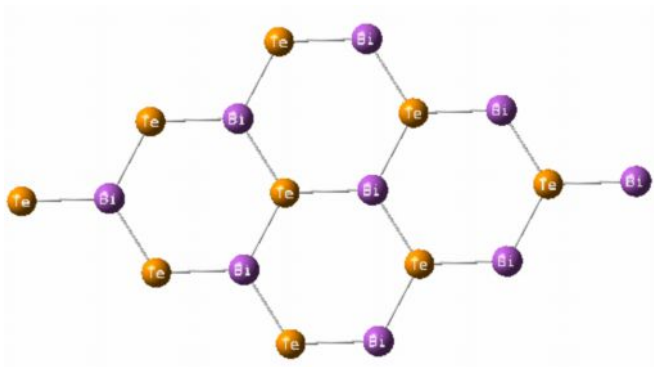


Figure. 1(e) Se substituted BiTe nanosheet

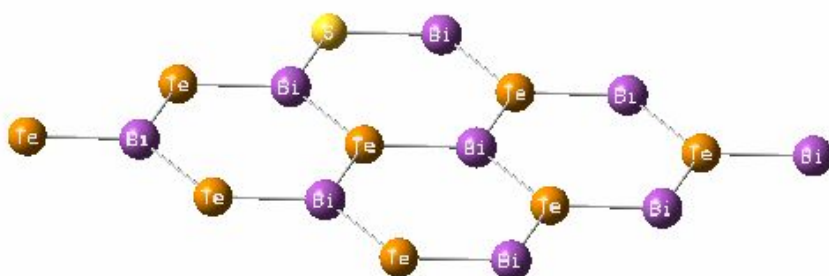


Figure. 1(f) S substituted BiTe nanosheet

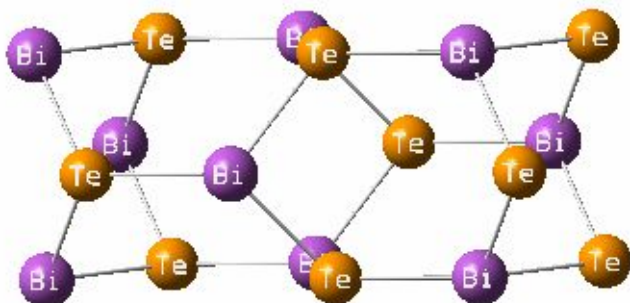


Figure. 1(g) pristine BiTe nanotube

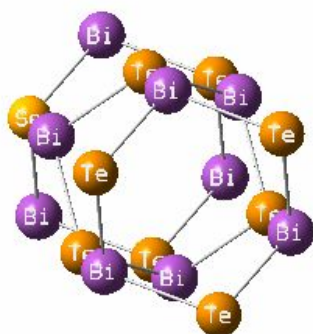


Figure. 1(h) Se substituted BiTe nanotube

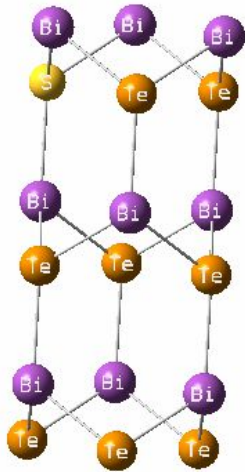


Figure. 1(i) S substituted BiTe nanotube

Table. 1 Formation energy, point symmetry and dipole moment of BiTe nanostructures

Nanostructures	Formation energy (eV)	Dipole moment (Debye)	Point Group
pristine BiTenocone	-39.44	7.03	C _s
Se substituted BiTenocone	-40.26	7.47	C ₁
S substituted BiTenocone	-41.07	7.49	C ₁
pristine BiTenosheet	-39.44	19.39	C _s
Se substituted BiTenosheet	-40.26	19.73	C _s
S substituted BiTenosheet	-40.26	20.34	C _s
pristine BiTe nanotube	-39.44	9.16	C ₁
Se substituted BiTe nanotube	-40.26	9.3	C _s
S substituted BiTe nanotube	-40.26	10.47	C _s

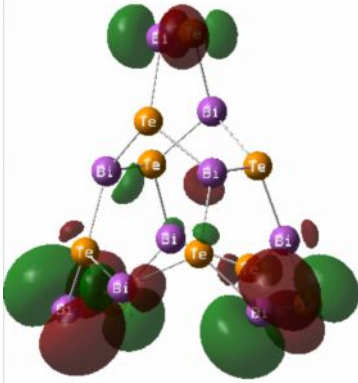
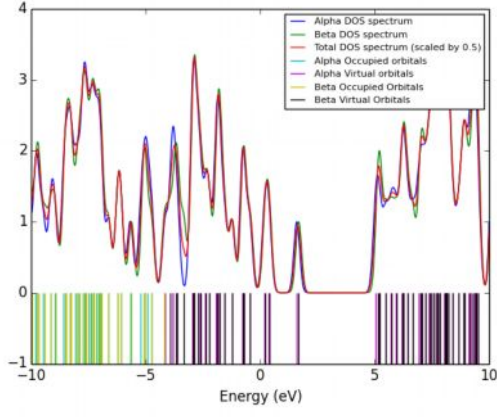
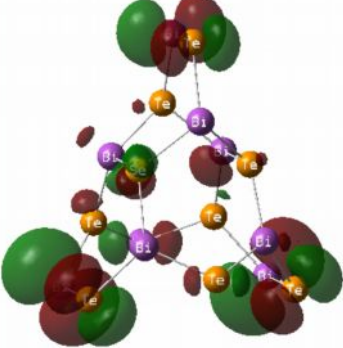
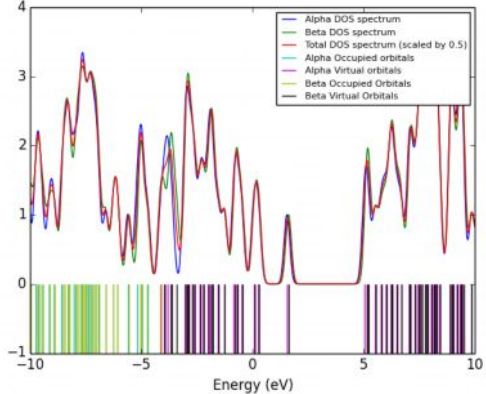
The structural stability of pristine, Se and S incorporated BiTe nanostructures are described using formation energy as shown in equation 1,

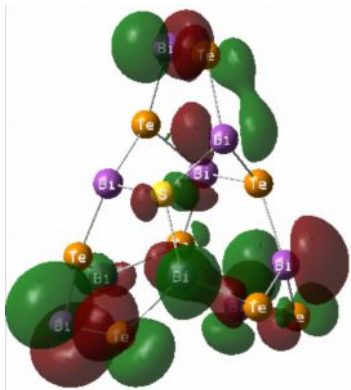
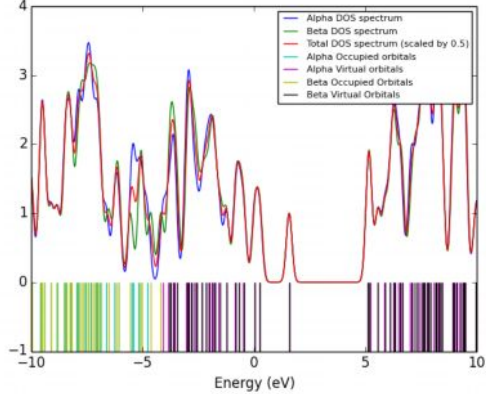
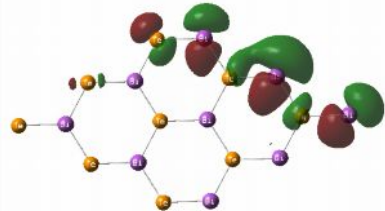
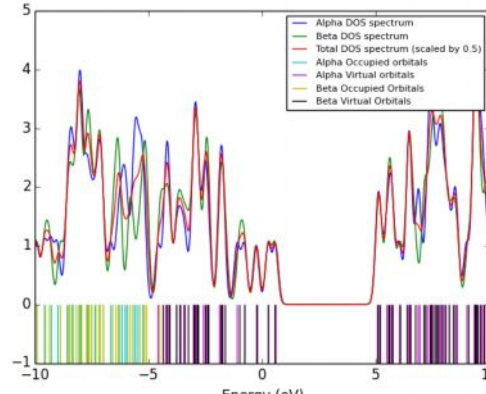
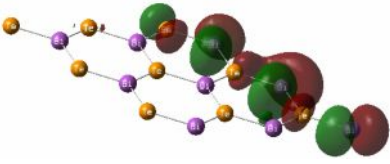
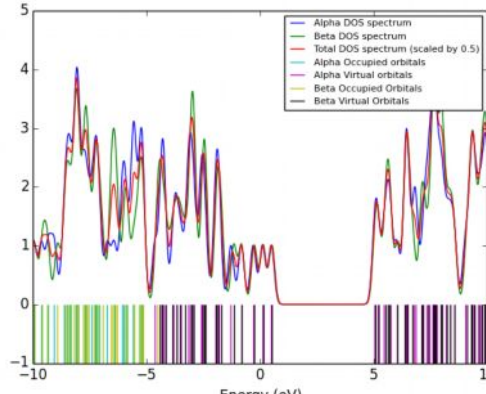
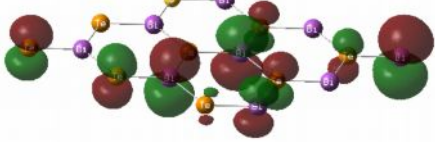
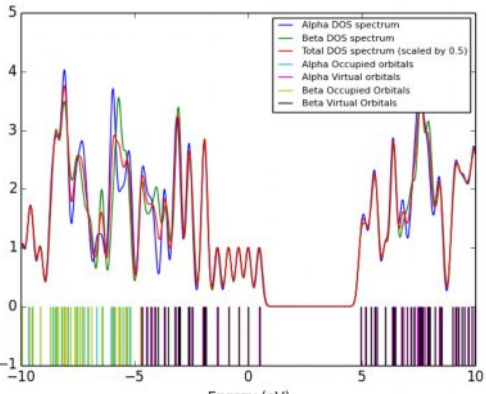
$$E_{\text{form}} = E(\text{BiTe nanostructure}) - xE(\text{Bi}) - yE(\text{Te}) - zE(\text{dopant}) \quad (1)$$

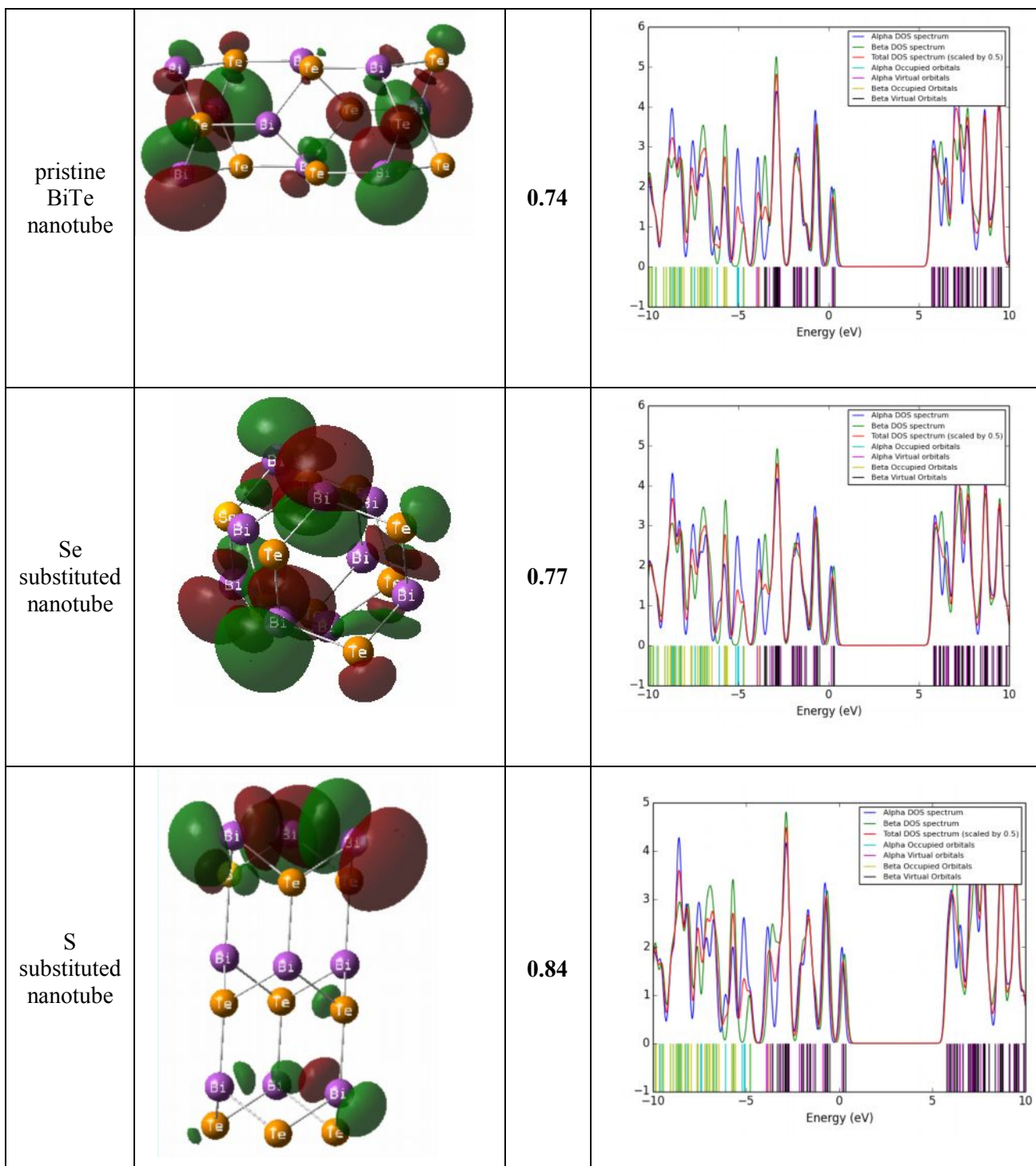
where $E(\text{BiTe nanostructure})$ refers the total energy of BiTe nanostructure, $E(\text{Bi})$, $E(\text{Te})$ and $E(\text{dopant})$ represents the corresponding energy of isolated Bi, Te and dopant atoms namely Se and S. Furthermore, x , y and z represents the total number of Bi, Te and dopant atoms respectively. The dipole moment, formation energy and point group of pristine, Se and S substituted BiTe nanostructures are tabulated in Table 1. The formation energy of pristine, Se and S substituted BiTenocones are -39.44, -40.26 and -41.07 eV respectively. Almost same value of formation energy is observed for pristine; Se and S substituted BiTe nanostructures. Moreover, the stability of BiTe nanostructure slightly increases due to substitution of Se and S atoms. Since, the formation energy of Se and S substituted BiTe nanostructures in the form of nanocone, nanosheet and nanotube are relatively large compared with pristine BiTe nanostructures. Besides, the S substituted BiTe nanostructures are more stable. The dipole moment of pristine, Se and S incorporated BiTenocones are 7.03, 7.47 and 7.49 Debye respectively. Similarly, the corresponding DP value of BiTenosheets and nanotubes are observed in the range of 19.39-20.34 and 9.16-10.47 Debye respectively. As a result, the uniform charge distribution is observed in BiTenocone compared with BiTenosheet and nanotube. The point group of BiTe nanostructures is found to be C_s and C₁. C₁ has only identity operation. C_s has identity and mirror plane symmetry.

The electronic properties of BiTe nanostructures can be discussed in terms of lowest unoccupied molecular orbital (LUMO) and highest occupied molecular orbital (HOMO) [26-29]. The energy gap values for pristine, Se and S substituted BiTe nanocone, nanosheet and nanotube are tabulated in Table 2. From the observation of energy gap, the incorporation of impurities influence the HOMO-LUMO gap compared with pristine BiTe nanosheet. The energy gap value for pristine, Se and S substituted BiTe nanosheet are 0.64, 0.54 and 0.47 eV respectively. This infers that the conductivity of BiTe nanosheet increases with the incorporation of Se and S atoms due to the decrease in HOMO-LUMO gap. In contrast, the conductivity of BiTe nanostructures slightly decreases with the incorporation of same Se and S impurities in nanocone and nanotube as shown in Table 2. The corresponding energy gap value for pristine, Se and S substituted nanocone are 0.58, 0.59 and 0.7 eV. In that order, the energy gap values for BiTe nanotube are 0.74, 0.77 and 0.84 eV. Thus, it is implied that the geometric structure and incorporation of dopant element plays a vital role in deciding the conductivity of BiTe nanostructure. The density of states spectrum and visualization of HOMO-LUMO gap for BiTe nanostructures are shown in Table 2. BiTe nanostructures exhibit semiconducting behavior with narrow band gap. Besides, less energy is required in moving the electrons from the valance band to the conduction band. As a result, the localization of charges is recorded to be more in BiTe LUMO level than in HOMO level. Owing to the influence of dopant atom, the density of charges in both HOMO and LUMO levels gets changed. Therefore, the electronic properties of BiTe nanostructures can be fine-tuned with the substitution of Se and S atoms.

Table. 2 HOMO –LUMO gap and density of states of BiTe nanostructures

Nanostructures	HOMO – LUMO Visualization 	E_g (eV)	HOMO, LUMO and DOS Spectrum
pristine BiTe nanocone		0.58	
Se substituted nanocone		0.59	

<p>S substituted nanocone</p>		<p>0.7</p>	
<p>pristine BiT nanosheet</p>		<p>0.64</p>	
<p>Se substituted nanosheet</p>		<p>0.54</p>	
<p>S substituted nanosheet</p>		<p>0.47</p>	



Ionization potential, electron affinity, chemical potential and chemical hardness of BiTe nanostructures

The electronic properties of BiTe nanostructure can also be described with electron affinity (EA) and ionization potential (IP) [30-33]. Figure 2 illustrates the EA and IP of BiTe nanostructures. Usually the amount of energy required in removing the electron from BiTe nanostructure is referred as IP and the variation in energy owing to addition of electrons in BiTe nanostructure is called as EA. Almost same trend is recorded for both EA and IP for different BiTe nanostructures as shown in Figure 2. Comparatively, more energy is required to remove electron from BiTenanosheet among others. Electron affinity plays an important role on both plasma physics and chemical sensors. The EA value for pristine, Se and S substituted BiTenanocones are 4.14, 4.11 and 4.08 eV respectively. Similarly, the electron affinity for BiTenanosheet and nanotube are shown in Figure 2. From the observation it inferred that the energy change is more for BiTenanosheet, which arise due to its

geometry of the structure. In contrast, comparatively less change in energy is observed for both BiTenanocone and nanotube. Moreover, two dimensional sheet structures give rise to more change in energy.

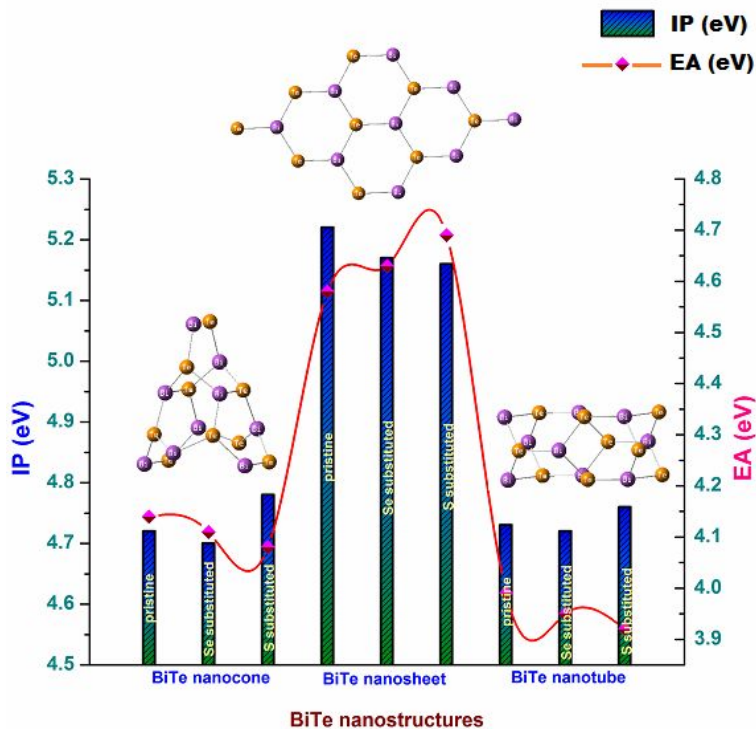


Figure.2 IP and EA of BiTe nanostructures.

The structural stability of BiTe nanostructures can also be described in terms of chemical potential and chemical hardness [34-37]. Chemical potential and chemical hardness for BiTe nanostructures can be calculated using the equation $\mu = -(\text{IP} + \text{EA})/2$ and $\eta = (\text{IP} - \text{EA})/2$ respectively as shown in Table 3. Almost same chemical potential are observed for BiTe nanostructures as shown in Table 3. Furthermore, there is not much variation observed in chemical hardness. In the case of BiTenanosheet, chemical hardness decreases with substitution of Se and S impurities. In contrast, the chemical hardness increases with the substitution of same dopant atom of Se and S in BiTenanocone and nanotube. It is inferred that the geometry of BiTe nanostructure plays a vital role in chemical hardness. The orbital overlapping of Bi, Te and dopant atoms gives rise to the variation in chemical hardness. Therefore, the structural stability of BiTe nanostructure also depends on the incorporation of dopants. The effect of CH and CP can also be discussed by effective fragment potential model, in most of the cases; the chemical hardness can also be depicted by electronegativity, which is one of the significant factors in semiconductor physics.

Table. 3 Chemical potential and chemical hardness of BiTe nanostructures

Nanostructures	Chemical potential (eV)	Chemical hardness (eV)
pristine BiTenanocone	-4.43	0.29
Se substituted BiTenanocone	-4.41	0.30
S substituted BiTenanocone	-4.43	0.35
pristine BiTenanosheet	-4.9	0.32
Se substituted BiTenanosheet	-4.9	0.27
S substituted BiTenanosheet	-4.92	0.24
pristine BiTe nanotube	-4.36	0.37
Se substituted BiTe nanotube	-4.34	0.39
S substituted BiTe nanotube	-4.34	0.42

Conclusion

The realistic nanostructure of pristine, Se and S incorporated BiTe nanostructures are simulated and optimized using DFT along with B3LYP/LanL2DZ basis set. The structural stability of BiTe nanostructures are investigated using formation energy, chemical hardness and chemical potential. Point symmetry and dipole moment of pure, Se and S substituted BiTe nanostructures are also reported. Using electron affinity, ionization potential, HOMO-LUMO gap and density of states spectrum, electronic properties of BiTe nanostructures are discussed. The findings of the present work are the structural stability and electronic properties of BiTe nanostructures can be fine-tuned with the incorporation of Se and S atom as impurities. Moreover, the electronic and structural properties of nanocone, nanosheet and nanotube form of BiTe nanostructure can be tailored with substitution impurity. The results of the work give the insights to enhance the electronic properties of BiTe, which find its potential application in thermoelectric materials.

References

1. Bubnova O, Khan Z U, Maltsev A, Braun S, Fahlman M, Berggren M and Crispin X., Optimization of the thermoelectric figure of merit in the conducting polymer poly(3,4-ethylenedioxythiophene), *Nat. Mater.*, 2011, 10, 429-433.
2. Zhao H Z, Pokheral M, Zhu G H, Chen S, Lukas K, Jie Q, Opeil C, Chen G and Ren Z F., Dramatic thermal conductivity reduction by nanostructures for large increase in thermoelectric figure-of-merit of FeSb₂, *Appl. Phys. Lett.*, 2011, 99, 163101.
3. Szczech J R, Higgins J M and Jin S., Enhancement of the thermoelectric properties in nanoscale and nanostructured materials, *J. Mater. Chem.*, 2011, 21, 4037-4055.
4. Yan X A, Poudel B, Ma Y, Liu W S, Joshi G, Wang H, Lan Y C, Wang D Z, Chen G and Ren Z F., Experimental Studies on Anisotropic Thermoelectric Properties and Structures of n-Type Bi₂Te_{2.7}Se_{0.3}, *Nano Lett.*, 2010, 10, 3373-3378.
5. Fukuda D, Kimura S and Endo M., Absolute energy reference calorimeter with bismuth telluride thermocouples for laser energy standard, *Rev. Sci. Instrum.*, 2005, 76, 113107.
6. Carmo JP, Silva MF, Ribeiro JF, Wolfenbittel RF, Alpuim P, Rocha JG, Goncalves LM and Correia JH., Digitally-controlled array of solid-state microcoolers for use in surgery, *Microsystem Technologies.*, 2011, 17, 1283-1291.
7. Bensaid S, Brignone M, Ziggioni A and Specchia S., High efficiency Thermo-Electric power generator, *International Journal of Hydrogen Energy.*, 2012, 37, 1385-1398.
8. Kalantar-Zadeh K, Wlodarski W, Li L, Kandasamy S and Rosengarten G., A thermoelectric transducer based on Bismuth Telluride thin films for H₂ gas sensing, *Journal of Rare Metal Materials and Engineering.*, 2006, 35, 190-194.
9. Mishra SK, Satpathy S and Jepsen O., Electronic structure and thermoelectric properties of bismuth telluride and bismuth selenide, *Journal of Physics: Condensed Matter.*, 1997, 9, 461-470.
10. Bourgault D, Garampon CG, Caillault N, Carbone L and Aymami JA., Thermoelectric properties of n-type Bi₂Te_{2.7}Se_{0.3} and p-type Bi_{0.5}Sb_{1.5}Te₃ thin films deposited by direct current magnetron sputtering, *Thin Solid Films.*, 2008, 516, 8579-8583.
11. Takashiri M, Miyazaki K and Tsukamoto H., Structural and thermoelectric properties of fine-grained Bi_{0.4}Te_{3.0}Sb_{1.6} thin films with preferred orientation deposited by flash evaporation method, *Thin Solid Films.*, 2008, 516, 6336-6343.
12. Kwon SD, Ju BK, Yoon SJ and Kim JS., Fabrication of Bismuth Telluride-Based Alloy Thin Film Thermoelectric Devices Grown by Metal Organic Chemical Vapor Deposition, *J. Electron. Mater.*, 2009, 38, 920-924.
13. Li FH and Wang W., Electrodeposition of Bi_xSb_{2-x}Te_y thermoelectric thin films from nitric acid and hydrochloric acid systems, *Appl. Surf. Sci.*, 2009, 255, 4225-4231.
14. Srinivasan R, Gothard N and Spowart J., Improvement in thermoelectric properties of an n-type bismuth telluride (Bi₂Se_{0.3}Te_{2.7}) due to texture development and grain refinement during hot deformation, *Materials Letters.*, 2010, 64, 1772-1775.
15. Zenga Z, Yanga P and Hua Z., Temperature and size effects on electrical properties and thermoelectric power of Bismuth Telluride thin films deposited by co-sputtering, *Applied Surface Science.*, 2013, 268, 472-476.

16. Molli M, Parola S, AvinashChunduri LA, Aditha S, SaiMuthukumarV, Rattan TM and Kamiseti V., Solvothermal synthesis and study of nonlinear optical properties of nanocrystalline thallium doped bismuth telluride, *Journal of Solid State Chemistry.*, 2012, 189, 85–89.
17. Nagarajan V and Chandiramouli R., DFT investigation on structural stability, electronic properties and CO adsorption characteristics on anatase and rutile TiO₂ nanostructures, *Ceram. Int.*, 2014, 40, 16147-16158. <http://dx.doi.org/10.1016/j.ceramint.2014.07.046>
18. Nagarajan V and Chandiramouli R., TeO₂ nanostructures as a NO₂ sensor: DFT Investigation, *Computational and Theoretical Chemistry*, 2014, 1049, 20-27.
19. Nagarajan V and Chandiramouli R., NiO nanostructure as a CO sensor: DFT investigation, *Struct. Chem.*, 2014, 25, 1765-1771.
20. Frisch M J et al., Gaussian, Inc., Wallingford CT, 2009.
21. Chandiramouli R., A DFT study on the structural and electronic properties of Barium Sulfide nanoclusters, *Res. J. Chem. Environ.*, 2013, 17, 64-73.
22. Nagarajan V and Chandiramouli R., Effect on the structural stability and electronic properties of impurity substituted sodium selenide nanostructures—A quantum chemical study, *Int.J. ChemTech Res.*, 2014, 6(4), 2240-2246.
23. Nagarajan V and Chandiramouli R., Investigation on the structural stability and electronic properties of InSb nanostructures – A DFT approach, *Alexandria Engineering Journal.*, 2014, 53, 437.
24. Srinivasaraghavan R, Chandiramouli R, Jeyaprakash BG and Seshadri S., Quantum chemical studies on CdO nanoclusters stability, *Spectrochim. Acta, Part A.*, 2013, 102, 242.
25. O'boyle NM, Tenderholt AL and Langner KM., A Library for Package+Independent Computational Chemistry Algorithms, *J. Comput. Chem.*, 2007, 29, 839.
26. Ganesan V, Nagarajan V, Saravanakannan V and Chandiramouli R., Quantum chemical insights on tuning structural stability and electronic properties of PdO nanostructures, *Int.J. ChemTech Res.*, 2014, 6(7), 3832.
27. Sriram S, Chandiramouli R, Balamurugan D and Thayumanvan A., A DFT study on the structural and electronic properties of ZnO nanoclusters, *Eur. Phys. J. Appl. Phys.*, 2013, 62, 30101.
28. Nagarajan V, Saravanakannan V and Chandiramouli R., Quantum Chemical Insights on Structural and Electronic properties of Anionic, Cationic and Neutral ZrO₂ nanostructures, *Int.J. ChemTech Res.*, 2014, 6(5), 2962-2970.
29. Nagarajan V and Chandiramouli R., Structural Stability and Electronic Properties of Neutral, Anionic and Cationic Cesium Chloride Nanostructures – A DFT Study, *Res J Pharm Biol Chem Sci.*, 2014, 5(1), 365-379.
30. Nagarajan V and Chandiramouli R., A quantum chemical exploration on structural stability and electronic properties of CdZnO nanostructures, *Der PharmaChemica.*, 2014, 6 (1), 37-46.
31. Nagarajan V and Chandiramouli R., Quantum Chemical Studies on ZrN Nanostructures, *Int.J. ChemTech Res.*, 2014, 6(1), 21-30.
32. Nagarajan V and Chandiramouli R., CO Adsorption Characteristics on Impurity Substituted In₂O₃ Nanostructures: A Density Functional Theory Investigation, *J Inorg Organomet Polym.*, 2015, 25, 837-847.
33. Nagarajan V and Chandiramouli R., DFT investigation on CO sensing characteristics of hexagonal and orthorhombic WO₃ nanostructures, *Superlattices Microstruct.*, 2015, 78, 22-39.
34. Chandiramouli R, Sriram S and Balamurugan D., Quantum chemical studies on (ZnO)_n/(NiO)_n heterostructured nanoclusters, *Mol. Phys.*, 2014, 112, 151-164.
35. Nagarajan V and Chandiramouli R., DFT investigation of formaldehyde adsorption characteristics on MgO nanotube, *J Inorg Organomet Polym.*, 2014, 24, 1038-1047.
36. Sriram S, Chandiramouli R and Jeyaprakash BG., Influence of fluorine substitution on the properties of CdO nanocluster: a DFT approach, *Struct Chem.*, 2014, 25, 389-401.
37. Ganesan V, Nagarajan V, Saravanakannan V and Chandiramouli R., Influence of substitution impurities on electronic properties of CaSe nanostructures – a quantum chemical study, *Int.J. ChemTech Res.*, 2014, 6 (7), 3822-3831.
